Inorganic Chemistry
Communication

Inorg. Chem. 2011, 50, 705–707 705
DOI: 10.1021/ic101731j

Homogeneous Photocatalytic Hydrogen Production Using π-Conjugated Platinum(II) Arylacetylide Sensitizers

Xianghuai Wang, Sébastien Goeb,‡ Zhiqiang Ji, Nadezhda A. Pogulaichenko, and Felix N. Castellano*

Department of Chemistry and Center for Photochemical Sciences, Bowling Green State University, Bowling Green, Ohio 43403, United States. ‡Present address: Université d Angers, CIMA UMR CNRS 6200-UFR Sciences, 2 Boulevard Lavoisier, 49045 Angers, France.

Received August 25, 2010

Three platinum(II) terpyridylacetylide charge-transfer complexes possessing a lone ancillary ligand systematically varied in phenylacetylide π-conjugation length, $[Pt(^tBu_3tpy)([C{\equiv}CC_6H_4]_nH)]ClO_4$ ($n = 1-3$), are evaluated as photosensitizers (PSs) for visible-light-driven ($\lambda > 420$ nm) hydrogen production in the presence of a cobaloxime catalyst and the sacrificial electron donor triethanolamine (TEOA). Excited-state reductive quenching of the PS by TEOA produces PS^- (k_q scales with the driving force as **1** > **2** > **3**), enabling thermal electron transfer to the cobalt catalyst. The initial H_2 evolution is directly proportional to the incident photon flux and visible-light harvesting capacity of the sensitizer, **3** > **2** > **1**. The combined data suggest that PSs exhibiting attenuated bimolecular reductive quenching constants with respect to the diffusion limit can overcome this deficiency through improved light absorption in homogeneous H_2-evolving compositions.

Hydrogen (H_2) derived from water represents a promising carbon-neutral and renewable solar-derived fuel suitably poised to accommodate select future global energy requirements while mitigating projected climate change. A variety of photocatalytic schemes continue to be broadly investigated for solar H_2 production.[1] In efforts to improve the photon-to-fuel efficiency in H_2 generation through proton reduction, many classes of homogeneous[2−10] and heterogeneous[11−17] compositions have been examined. Cobalt diglyoxime catalysts,[18,19] vitamin B_{12} structural mimics,[20] are particularly promising candidates for solar-driven water reduction because the critical fuel-forming cobalt(III) hydride intermediate is readily produced from electron transfer initiated from an appropriate excited-state photosensitizer (PS) in the presence of a proton donor.[21] The $[Pt(ttpy)(C{\equiv}CPh)]^+$ complex, where ttpy is 4′-tolylterpyridine, has demonstrated the potential for harvesting high-energy visible light in solar H_2 research because its excited-state redox properties are amenable to H_2 photocatalysis.[6,12,22,23] In conjunction with the cobalt(III) diglyoxime complex $[Co(dmgH)_2pyCl]$,[24] this and several related platinum(II) PSs have been shown to be more effective at producing H_2 with respect to other cobalt diglyoxime catalysts in water/organic solvent mixtures.[6,22,25] On the basis of current accumulated knowledge, we decided to utilize a three-component reductive quenching strategy [platinum(II) PS, $[Co(dmgH)_2pyCl]$, catalyst; triethanolamine (TEOA), sacrificial electron donor] to examine the factors influencing

*To whom correspondence should be addressed. E-mail: castell@bgsu.edu.

(1) Esswein, A. J.; Nocera, D. G. *Chem. Rev.* **2007**, *107*, 4022–4047.
(2) Cline, E. D.; Adamson, S. E.; Bernhard, S. *Inorg. Chem.* **2008**, *47*, 10378–10388.
(3) Yamauchi, K.; Masaoka, S.; Sakai, K. *J. Am. Chem. Soc.* **2009**, *131*, 8404–8406.
(4) Fihri, A.; Artero, V.; Pereira, A.; Fontecave, M. *Dalton Trans.* **2008**, 5567–5569.
(5) Fihri, A.; Artero, V.; Razavet, M.; Baffert, C.; Leibl, W.; Fontecave, M. *Angew. Chem., Int. Ed.* **2008**, *47*, 564–567.
(6) Du, P.; Schneider, J.; Luo, G.; Brennessel, W. W.; Eisenberg, R. *Inorg. Chem.* **2009**, *48*, 4952–4962.
(7) Elvington, M.; Brown, J.; Arachchige, S. M.; Brewer, K. J. *J. Am. Chem. Soc.* **2007**, *129*, 10644–10645.
(8) Probst, B.; Kolano, C.; Hamm, P.; Alberto, R. *Inorg. Chem.* **2009**, *48*, 1836–1843.
(9) Probst, B.; Rodenberg, A.; Guttentag, M.; Hamm, P.; Alberto, R. *Inorg. Chem.* **2010**, *49*, 6453–6460.
(10) McCormick, T. M.; Calitree, B. D.; Orchard, A.; Kraut, N. D.; Bright, F. V.; Detty, M. R.; Eisenberg, R. *J. Am. Chem. Soc.* **2010**, *132*, 15480–15483.
(11) Curtin, P. N.; Tinker, L. L.; Burgess, C. M.; Cline, E. D.; Bernhard, S. *Inorg. Chem.* **2009**, *48*, 10498–10506.
(12) Du, P.; Schneider, J.; Li, F.; Zhao, W.; Patel, U.; Castellano, F. N.; Eisenberg, R. *J. Am. Chem. Soc.* **2008**, *130*, 5056–5058.
(13) Zong, X.; Na, Y.; Wen, F.; Ma, G.; Yang, J.; Wang, D.; Ma, Y.; Wang, M.; Sun, L.; Li, C. *Chem. Commun.* **2009**, 4536–4538.
(14) Zhang, J.; Du, P.; Schneider, J.; Jarosz, P.; Eisenberg, R. *J. Am. Chem. Soc.* **2007**, *129*, 7726–7727.
(15) Streich, D.; Astuti, Y.; Orlandi, M.; Schwartz, L.; Lomoth, R.; Hammarstroem, L.; Ott, S. *Chem.—Eur. J.* **2010**, *16*, 60–63.
(16) Zhang, P.; Wang, M.; Na, Y.; Li, X. Q.; Jiang, Y.; Sun, L. C. *Dalton Trans.* **2010**, *39*, 1204–1206.
(17) Tinker, L. L.; Bernhard, S. *Inorg. Chem.* **2009**, *48*, 10507–10511.
(18) Dempsey, J. L.; Winkler, J. R.; Gray, H. B. *J. Am. Chem. Soc.* **2010**, *132*, 1060–1065.
(19) Dempsey, J. L.; Brunschwig, B. S.; Winkler, J. R.; Gray, H. B. *Acc. Chem. Res.* **2009**, *42*, 1995–2004.
(20) Schrauzer, G. N. *Acc. Chem. Res.* **1968**, *1*, 97–103.
(21) Chao, T.-H.; Espenson, J. H. *J. Am. Chem. Soc.* **1978**, *100*, 129–133.
(22) Du, P.; Knowles, K.; Eisenberg, R. *J. Am. Chem. Soc.* **2008**, *130*, 12576–12577.
(23) Du, P.; Schneider, J.; Jarosz, P.; Eisenberg, R. *J. Am. Chem. Soc.* **2006**, *128*, 7726–7727.
(24) Razavet, M.; Artero, V.; Fontecave, M. *Inorg. Chem.* **2005**, *44*, 4786–4795.
(25) Lazarides, T.; McCormick, T.; Du, P.; Luo, G.; Lindley, B.; Eisenberg, R. *J. Am. Chem. Soc.* **2009**, *131*, 9192–9194.

Published on Web 01/04/2011

Table 1. Room Temperature Photophysical Properties and Excited-State Electron-Transfer Rate Constants of **1**−**3** in 1:1 Acetonitrile/Water

compound	λ_{em} (nm)	E^{*red} (V vs Fc^+/Fc)[a]	ϕ_{em}[b−d]	τ_{em}[c](ns)	k_r[e] (s^{-1})	k_{nr}[f] (s^{-1})	k_{ox}[g] (M^{-1} s^{-1})	k_{red}[h] (M^{-1} s^{-1})
1	583	1.00	0.016	508	3.1×10^4	1.9×10^6	2.92×10^9	1.16×10^9
2	592	0.96	0.0088	246	3.6×10^4	4.0×10^6	3.14×10^9	5.51×10^8
3	592	0.86	0.016	390	4.1×10^4	2.5×10^6	3.70×10^9	4.92×10^8

[a] The excited-state reduction potential (vs Fc^+/Fc) is calculated as $E^*_{1/2}{}^{red} = E^*_{1/2}{}^{red} + E_{0-0}$ with E_{0-0} obtained from the 77 K emission spectra measured in 4:1 ethanol/methanol (see the SI). [b] The quantum yield of photoluminescence measured relative to $[Ru(bpy)_3](ClO_4)_2$ ($\phi_{em} = 0.062$) in acetonitrile. [c] Emission quantum yields and lifetime decays, ±5%. [d] $\eta_{ACN} = 1.3422$ and $\eta_{ACN/H_2O} = 1.3454$.[27] [e] $k_r = \phi/\tau$. [f] $k_{nr} = (1 - \phi)/\tau$. [g] Oxidative quenching by the $[Co^{III}(dmgH)_2pyCl]$ catalyst. [h] Reductive quenching by TEOA.

Chart 1. Molecular Structures of the Platinum(II) Terpyridyl π-Conjugated Arylacetylide PSs

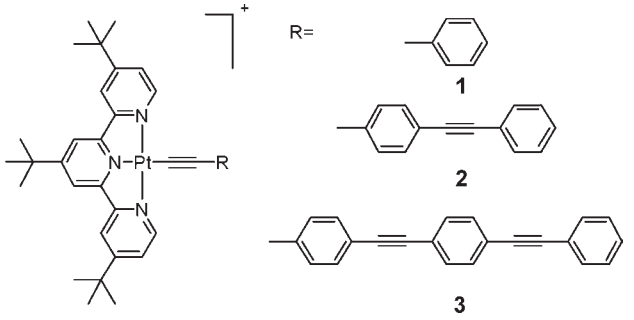

H_2 production from a series of π-conjugated platinum(II) arylacetylide sensitizers (Chart 1).

Compounds **1**−**3** were available from a previous study that revealed that the charge-transfer (CT) excited states in these complexes transiently produce an arylacetylide-localized "hole" responsible for most of the excited-state absorptions, which progressively red-shift across the series.[26] Each structure features the $^tBu_3$tpy ligand, ultimately responsible for driving catalyst reduction in all instances. The first reduction of these complexes is indeed $^tBu_3$tpy ligand-based, occurring at the same potential within experimental error (±20 mV) as that measured by differential pulse voltammetry, −1.39 V versus the Fc^+/Fc internal standard. Under the same experimental conditions, $[Pt(ttpy)(C{\equiv}CPh)]^+$ exhibits a one-electron reduction at −1.27 V. The CT absorption profiles across the series are quite similar, and the extinction coefficients increase concomitant with the phenylacetylide conjugation length.[26] The benchmark 4′-tolylterpyridylplatinum(II) phenylacetylide PS exhibits slightly superior low-energy light harvesting with respect to **1** and **2**; however, **3** exhibits the highest oscillator strength among the molecules in this study. The excited-state reduction potentials of **1**−**3** calculated from the 77 K emission spectra and one-electron reduction potentials are collected in Table 1 (**1** > **2** > **3**). Because the present study utilized a 1:1 CH_3CN/water solvent composition, excited-state lifetimes, quantum yields, and reductive (TEOA) and oxidative $[Co(dmgH)_2pyCl]$ quenching rate constants for each sensitizer were determined using dynamic Stern−Volmer plots whose data are also compiled in Table 1. Both quenching processes approach diffusion limits across all sensitizers, with the oxidative process being faster in all instances. Armed with this knowledge, the H_2 photogeneration experiments were designed to optimize the reductive quenching pathway by using high concentrations of TEOA (0.5 M), thereby ensuring a more favorable thermodynamic driving force for cobaloxime catalyst reduction. The reductive quenching rates follow the same trend as the corresponding excited-state potentials: **1** > **2** > **3** (Table 1).

H_2 photocatalysis experiments utilized 50 mL of 1:1 CH_3CN/H_2O (v/v) containing 1.1×10^{-5} M PS, 2.0×10^{-4} M $[Co(dmgH)_2pyCl]$, and 0.5 M TEOA combined in a 100 mL Pyrex round-bottomed flask vigorously agitated with a magnetic stirrer. The pH was adjusted to 8.5 with a 2.5 M HCl stock solution; this pH was selected based on previously established optimizations for the catalytic action of related PS compositions.[22] Each sample was irradiated using a 300 W Xe arc lamp equipped with a circulating water filter and a 420-nm-long pass filter. The reaction flask is connected to a closed-loop direct-injection gas chromatography system equipped with a 5 Å molecular sieve column and a thermal conductivity detector as described previously.[12] Figure 1 presents H_2 photogeneration ($\lambda > 420$ nm) plotted in turnover number (TON; moles of H_2 per moles of sensitizer) measured as a function of the irradiation time for compounds **1**−**3** and $[Pt(ttpy)(C{\equiv}CPh)]^+$. The latter is used as a primary H_2 photogeneration standard for which side-by-side quantitative comparisons can be performed. In all cases, an induction period between 10 and 20 min is observed (Figure 1, inset), which is presumably related to the combined effect of converting cobalt(III) to cobalt(II), which is mandated prior to any catalytic action and solvent saturation with H_2. Under our experimental conditions, **1**−**3** and $[Pt(ttpy)(C{\equiv}CPh)]^+$ continuously produce H_2 for up to ∼3−4 h, with **3** exhibiting the largest overall TON of 789. It is important to note that these photocatalytic mixtures are operating under photon flux control at early photolysis times because the total H_2 produced is linear with the incident light power density. The same compositions exposed to monochromatic excitation at 442 nm (HeCd laser) all produce experimentally indistinguishable 1 h integrated quantum efficiencies for H_2 evolution, assuming that two electrons are generated per absorbed photon, $\Phi(H_2) = 0.16 \pm 0.01$; see Table 2 for details. The data presented in Figure 1 clearly demonstrate the trend of increasing initial H_2 production rate across the series as **1** < **2** < **3**, opposite that of the reductive quenching rates. We observe an identical trend, albeit with smaller initial rates and lower overall TONs, when the TEOA concentration is lowered by a factor of 10 to 0.05 M. From these combined experimental results, it immediately becomes clear that reduction of the PS is rate-limiting H_2 evolution. We believe that the relative H_2 production trend of **1** < **2** < **3** is largely a manifestation of increasing visible-light harvesting across the series as the long-wavelength extinction coefficients increase with increasing ancillary ligand conjugation length. These observations are consistent with recent results from the Detty and Eisenberg laboratories, which demonstrated an increased initial rate of H_2 evolution from the same cobaloxime

(26) Wang, X. H.; Goeb, S.; Ji, Z. Q.; Castellano, F. N. *J. Phys. Chem. B* **2010**, *114*, 14440–14449.

Table 2. Quantum Yields of H_2 Generation by **1**−**3** in 1:1 Acetonitrile/Water over 1 h of Continuous 442 nm Photolysis[a]

	α	ε^b	c (μM)^c	I_0 (mW)^d	I_{abs} (mW)^e	H_2 (μmol)^f	PS (μmol)^g	photons (μmol)^h	$\Phi(H_2)^i$	TON^j
1	0.048	4335	11	72.4	8.1	18.4	0.275	108	0.17	67
2	0.064	5837	11	73.4	10.9	23.9	0.275	145	0.16	87
3	0.103	9377	11	72.7	16.5	32.9	0.275	219	0.15	120

[a] Solutions prepared with 25 mL of total volume having a concentration of 1.1×10^{-5} M for complexes **1**−**3** containing 2×10^{-4} M cobaloxime and 0.5 M TEOA, with the pH adjusted to 8.5 and vigorously agitated with magnetic stirring; excitation was afforded by the isolated 442 nm line of a HeCd laser, and the entire path length is 2.5 cm. [b] Extinction coefficient (ε) of complexes **1**−**3** at 442 nm. [c] The concentration of the platinum(II) complex measured in a 1 cm path length cell, $c = \alpha/\varepsilon$. [d] Incident 442 nm laser power. [e] Total laser power absorbed by the PS. [f] Moles of H_2 produced. [g] Initial moles of the platinum(II) complex present in the solution. [h] Total moles of photons absorbed. [i] The quantum yield is the moles of H_2 produced ($^1/_2$ H_2 per photon) divided by the moles of photons absorbed assuming two electrons per incident photon by TEOA.[9] [j] H_2 turnovers produced in 1 h of 442 nm photolysis, TON = moles of H_2 produced/initial moles of PS present.

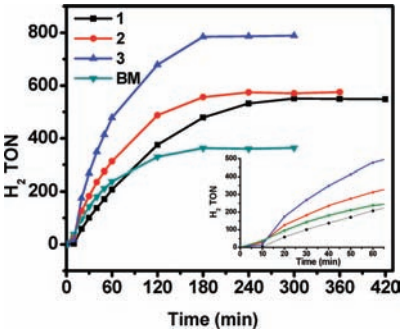

Figure 1. TON of H_2 vs PSs **1**−**3** and the $[Pt(ttpy)(C{\equiv}CPh)]^+$ benchmark (BM) obtained in the photocatalysis reaction with continuous irradiation ($\lambda > 420$ nm). Reaction composition: 1:1 CH_3CN/water (v/v) at pH 8.5 containing 1.1×10^{-5} M sensitizer, 2.0×10^{-4} M $[Co(dmgH)_2pyCl]$, and 0.5 M TEOA.

catalyst used here in conjunction with increasing *S*-rhodamine PS concentration.[10]

All of the present solution compositions unfortunately suffer from complete system degradation similar to that experienced previously when using dmg-based cobaloxime catalysts in reductive quenching-based photocatalytic schemes.[10,25] Following a brief induction period, the plots in Figure 1 quickly degenerate from a linear H_2-production slope into rates that continually decrease with the photolysis time. In all cases, the photocatalytic action ceases to function after several hours of continuous irradiation and the addition of 2 mL of mercury at the onset of photolysis, which suppresses any potential heterogeneous catalytic sites such as colloidal platinum or cobalt,[28] does not influence the H_2 evolution rate or total TON observed in experiments performed with **3** (Figure S5 in the SI). Related behavior has already been observed in $[Pt(ttpy)(C{\equiv}CPh)]^+$-based photocatalysis reactions in conjunction with cobaloximes,[6] leaving little doubt that H_2 generation in the present study is indeed completely homogeneous in nature. Control experiments verified that all three components were required for the observation of H_2 evolution, and the deletion of any single entity led to no appreciable H_2 production. Once catalytic activity ceased, the addition of fresh sensitizer revitalized H_2 photogeneration but only to ~25% of its initial turnover frequency. This indicates that both operational components decomposed during photolysis but enough cobaloxime remained intact to restart H_2 evolution. We note that cobalt catalyst decomposition can be partially slowed by the addition of excess $dmgH_2$,[10,25] which would lead to more net H_2 produced overall, i.e., higher total TON. At present, the chemical nature of the collective decomposition products remains unknown. However, control experiments confirm that complete PS decomposition, easily visualized by complete solution decolorization, occurs under photocatalytic conditions in the absence of cobaloxime, indicative of a potential competitive branching point in the reaction loop.[10] This finding suggests that, during the course of the reaction in the operational H_2-producing composition, cobaloxime decomposition with time will necessarily lead to PS^- decomposition when the latter can no longer transfer its transiently trapped high-potential-energy electron to an appropriate acceptor. In essence, PS decomposition becomes competitive with thermal electron transfer to the catalyst, resulting in rapid deterioration in H_2 evolution.[10] We note that partial photocatalytic activity can be restored upon the addition of fresh cobaloxime to the various reaction mixtures when H_2 evolution wanes, prior to complete solution decolorization. The combined results for these platinum(II) sensitizers parallel recent findings in corresponding *S*-rhodamine/cobaloxime compositions, leading us to invoke the identical mechanism,[10] although our data cannot distinguish between homolytic and heterolytic pathways for the actual H_2-releasing event from the cobalt catalyst.[18,19]

We have reported three efficient homogeneous catalytic systems enabling visible-light-driven hydrogen production from aqueous solutions using π-conjugated platinum(II) arylacetylide sensitizers in concert with a select cobaloxime catalyst. The stability of the present compositions appears to correlate to the ability for PS^- to electron transfer to the catalyst prior to its decomposition in addition to instabilities related to the catalyst. To better elucidate the relative PS performance in H_2 evolution, more stable catalysts are required to avoid complications resulting from coupled degradation processes. This work also illustrates that PSs exhibiting attenuated bimolecular reductive quenching constants with respect to the diffusion limit can overcome this deficiency through improved light absorption in homogeneous H_2-evolving compositions. This study advocates further exploration of sensitizer and catalyst designs in the hopes of understanding and improving upon current state-of-the-art water reduction photocatalytic schemes.

Acknowledgment. This research was supported by the National Science Foundation (Grant CHE-0719050), the Air Force Office of Scientific Research (Grant FA9550-05-1-0276), and the BGSU Research Enhancement Initiative.

Supporting Information Available: Additional data and details regarding all experimental procedures and techniques. This material is available free of charge via the Internet at http://pubs.acs.org.

(27) Openhaim, G.; Grushka, E. *J. Chromatogr. A* **2002**, *942*, 63–71.
(28) Anton, D. R.; Crabtree, R. H. *Organometallics* **1983**, *2*, 855–859.